

Inelastic scattering of low-energy electrons in liquid water computed from optical-data models of the Bethe surface

D. Emfietzoglou¹, I. Kyriakou¹, I. Abril², R. Garcia-Molina³ & H. Nikjoo⁴

¹Medical Physics Laboratory, University of Ioannina Medical School, Ioannina, Greece, ²Departament de Física Aplicada, Universitat d'Alacant, Alacant, Spain, ³Departamento de Física - CIOyN, Universidad de Murcia, Murcia, Spain, and ⁴Radiation Biophysics Group, Department of Oncology-Pathology, Karolinska Institute, Stockholm, Sweden

Abstract

Purpose: We provide a short overview of optical-data models for the description of inelastic scattering of low-energy electrons (10–10,000 eV) in liquid water. The effect on the inelastic scattering cross section due to different optical data and extension algorithms is examined with emphasis on some recent developments.

Materials and methods: The optical-data method whereby experimental optical data and theoretical extension algorithms are used to describe the dependence of the dielectric response function on energy- and momentum-transfer and obtain the Bethe surface of the material, currently represents the most used method for computing the inelastic scattering of low-energy electrons in condensed media. Two sets of experimental optical data for liquid water obtained from reflectance and inelastic X-ray scattering spectroscopy, respectively, and the extension algorithms of Ritchie, Penn, and Ashley are examined. Recent developments are discussed along with the role of corrections to the random phase approximation (RPA) of electron gas theory.

Results: The inelastic scattering cross section in the energy range 200–10,000 eV was found to be rather insensitive (to within 10%) to the choice of optical data or the extension algorithm. In contrast, differences between model calculations increase rapidly below 200 eV with the influence of the extension algorithm being dominant.

Conclusion: The choice of the extension algorithm used to extrapolate optical data to finite momentum transfer and obtain the Bethe surface is crucial in modelling the inelastic scattering of electrons with energies below 200 eV. A new set of measurements on the dielectric response function of liquid water beyond the optical limit and the development of extension algorithms that will go beyond RPA by considering the effect of (short-range) electron exchange and correlation should be of some priority.

Keywords: Inelastic scattering, low energy electron, liquid water, optical data, Bethe surface

Introduction

The inelastic scattering of low-energy electrons in liquid water is of great importance to understanding radiation action in cells, which contain 70–80% water in the condensed phase (mainly in liquid-like form). We define here as low-energy electrons those electrons with kinetic energy ranging from ~10 eV to ~10 keV. These electrons are most relevant to radiation effects studies because the probability of (non-radiative) inelastic collisions becomes largest in the energy range between 50–150 eV, while the (average) distance between inelastic collisions (the inelastic mean free path) is generally in the sub-micrometer scale (~1–100 nm), comparable to the dimensions of critical biological targets (DNA, chromosome, etc.). Since the majority of secondary electrons generated in ionization collisions have sub-keV energies, the present work should also be relevant to modeling the energy deposition around the tracks of energetic ions (e.g., protons, carbon ions).

Despite the importance of low-energy electrons, experimental data for their inelastic scattering in condensed media (including liquid water) are generally lacking, thus, model calculations are often the only source of information. The dielectric description of inelastic scattering, first introduced by Fermi (1940) in his classical treatment of the density effect in the stopping power of condensed media for relativistic charged particles, has been perhaps most useful in this context. The quantum mechanical formulation was advanced in the 1950s as summarized by Ritchie (1959), who has been one of the key contributors to the development and application of the optical-data method. The latter currently represents the most used approach for 'practical' calculations of inelastic scattering in condensed media (Fernández-Varea et al. 2005a). It is also considered the most convenient and reliable approach for modelling inelastic scattering in Monte Carlo particle transport simulation codes for condensed media (Dingfelder 2006, Salvat and Fernández-Varea 2009). The use of experimental optical data to model the

inelastic scattering of electrons in solids was first suggested by Powell (1967, 1974). This suggestion led to the development of the widely-used optical-data models of Ritchie (Hamm et al. 1975, Ritchie and Howie 1977), Penn (1987), and Ashley (1988) whereby experimental optical data and theoretical so-called extension algorithms (Fernández-Varea et al. 1992, 1993) are used to obtain the dependence of the dielectric function (or the energy-loss function) on energy- and momentum-transfer, respectively. Importantly, contrary to *ab initio* methods which are suitable only for very-low-energy electrons (below ~ 50 eV), optical-data models can work well over the wide energy range of practical interest.

We provide here a short overview of optical-data models used to compute the inelastic scattering of *low-energy* electrons in liquid water without considerations of exchange and low-energy (Coulomb) corrections. The use of the optical-data method at *relativistic* electron energies has been recently discussed by Fernández-Varea et al. (2005b).

Materials and methods

The energy- loss function

The optical-data method is based on the theoretical framework of the plane-wave Born approximation (PWBA) whereby, in the non-relativistic limit, the doubly-differential inelastic scattering cross section in energy (W) and momentum (q) transfer is given by:

$$\frac{d^2\Lambda}{dWdq} = \frac{1}{\pi a_0 T} \frac{1}{q} \text{Im} \left[\frac{-1}{\epsilon(W, q)} \right] \quad (1)$$

with $\text{Im}[\]$ denoting the imaginary part of the argument, a_0 being the Bohr radius (approximately 0.529 angstrom), T the electron kinetic energy, Λ the inelastic cross section in units of reciprocal length (also known as the *inverse inelastic mean free path*) and $\epsilon(W, q)$ the dielectric response function. The latter is a complex-valued function with its real and imaginary parts related to the screening and absorption properties of matter, respectively. The usefulness of the PWBA stems from the factorization of Eq. (1) into a particle-dependent factor and a material-dependent factor, which contains all the interesting properties of the target. It follows that inelastic scattering is completely determined by $\text{Im}[-1/\epsilon(W, q)]$, the so-called energy-loss function (ELF). Thus, inelastic scattering within the PWBA is essentially computed from simple quadratures of $\text{Im}[-1/\epsilon(W, q)]$ over the W - q plane. The latter defines a three-dimensional plot also known as the Bethe surface of the material. Equivalent descriptions of Eq. (1) are obtained using other materials functions such as the dynamic form factor or the generalized oscillator strength which bear a direct relation to the ELF (Inokuti 1971). For Eq. (1) to hold the incident electron energy (T) must be large compared to the binding energy (B) of the struck electron; as a rule of thumb $T > 10 B$. For the valence electrons, a representative value for B is the (nominal) plasmon energy of the material, E_{pl} . For liquid water $E_{pl} \approx 20$ eV, thus, Eq. (1) should hold for $T > 200$ eV. On the other hand, the widely-used Tanuma-Powell-Penn (TPP) predictive formula (Tanuma et al. 2011) suggests that the

optical-data method might be reliable down to ~ 50 eV. Moreover, with the addition of suitable exchange and low-energy (Coulomb) corrections, the optical-data method is routinely used even down to ~ 10 eV with reasonable success.

Optical data

Presently there exist two experimental optical data sets for liquid water that extend over a sufficient part of the valence excitation spectrum. The first set is that of the Oak Ridge group (Heller et al. 1974) that provides, via reflectance measurements on liquid water surfaces, the real refractive index (n) and the extinction coefficient (κ) of the complex index of refraction $\tilde{n} = n + i\kappa$ over the excitation range from 7.6–25.6 eV. The ELF at the optical limit is then obtained from:

$$\text{Im} \left[\frac{-1}{\epsilon(W, q \approx 0)} \right] = \text{Im} \left[\frac{-1}{(n + i\kappa)^2} \right] = \frac{2n\kappa}{(n^2 - \kappa^2)^2 + (2n\kappa)^2} \quad (2)$$

For more than 25 years the Oak Ridge data were the sole source of information on the dielectric response of liquid water in the vacuum ultraviolet range. The second set of optical data is that of the Sendai group (Hayashi et al. 2000) who measured, via inelastic X-ray scattering (IXS) spectroscopy, the generalized oscillator strength (GOS) of liquid water up to 160 eV excitation energy at nearly vanishing momentum transfer ($q \approx 0$). The ELF at the optical limit is then obtained from:

$$\text{Im} \left[\frac{-1}{\epsilon(W, q \approx 0)} \right] = \frac{\pi E_{pl}^2}{2W} \frac{df(W, q \approx 0)}{dW} \quad (3)$$

with $df(W, q \approx 0)/dW$ being the GOS at $q \approx 0$.

Extension algorithm

For a description of the Bethe surface which will enable inelastic calculations via Eq. (1) the ELF must be known for arbitrary momentum-transfer (i.e., $q \neq 0$). Measurements at $q \neq 0$ have been carried out in the late 1990s by the Sendai group (Watanabe et al. 2000) via IXS spectroscopy in the range $0.359 \leq q/\hbar \leq 6.786 \text{ \AA}^{-1}$. Since the experimental data cover a rather limited q -range, it is the role of theory to furnish a description of the ELF over the complete Bethe surface. The scheme used for extrapolating optical data to $q \neq 0$ is known as the ‘extension algorithm’ (Fernández-Varea et al. 1992, 1993). In the simplest case, an extension algorithm is a dispersion relation, i.e., an analytic expression of energy-transfer as a single-valued function of momentum-transfer. The homogeneous electron gas (EG) theory is commonly used to obtain a suitable extension algorithm (or dispersion relation). Despite being a theory of intra-band (rather than inter-band) excitations, the EG theory can be used (with negligible error) as an extension algorithm of the valence-electron excitations even for materials with a finite band-gap (e.g., insulators) since the latter is typically much smaller than the incident electron kinetic energy (Fernández-Varea et al. 1993). Obviously, the application of EG theory to core-electron excitations which have a large excitation threshold (typically > 100 eV) is problematic and

should be avoided in cases where the inner shells play an important role (e.g., in stopping power).

Several extension algorithms have been discussed in the literature. The earliest one is that of Ritchie and co-workers (Hamm et al. 1975, Ritchie and Howie 1977) where central role plays the so-called extended-Drude function:

$$D_i(W, q; E_i, \gamma_i) \equiv \frac{W \gamma_i(q)}{[E_i^2(q) - W^2]^2 + [W \gamma_i(q)]^2} \quad (4)$$

with E_i and γ_i denoting the position and width (or damping) of the i th Drude peak and $E_i(q)$ and $\gamma_i(q)$ their dispersion. In the earliest version (Hamm et al. 1975) a modified Drude (or Lorentz) model of interband excitations is employed leading to the expression:

$$\text{Im}\varepsilon(W, q) \equiv \varepsilon_2(W, q) = E_{pl}^2 \sum_i f_i(q) D_i(W, q; E_i, \gamma_i) \quad (5)$$

where ε_2 denotes the imaginary part of the dielectric function and the weighting factors $f_i(q)$ can be obtained from an empirical parameterization of the GOS of H_2O (Hamm et al. 1975). In subsequent work (Ritchie et al. 1978, 1991), a derivative form of Eq. (4) was employed for improving the asymptotic trends at large excitation energies W . The values of the model parameters $\{f_i, E_p, \gamma_i\}$ at $q = 0$ are obtained via a fit to the experimental optical data, i.e., by the condition $\varepsilon_2(W, q = 0)_{\text{model}} \approx \varepsilon_2(W, q \approx 0)_{\text{exp}}$. The Kramers-Kronig relation (Smith 1985) is then used to obtain the real part of the dielectric function which, owing to the form of the Drude function, can also be expressed analytically. The benefit of starting from $\text{Im}(\varepsilon)$ instead of $\text{Im}(-1/\varepsilon)$ is that it allows information on the excitation of the free molecule to be transferred in the condensed phase given that $\varepsilon_2(W, q = 0)$ can be partitioned to the principal absorption modes of the system. An alternative version of the extended-Drude model (Ritchie and Howie 1977) uses a generalized plasmon-pole model of ‘bound’ plasmons from different sub-bands to express the ELF in the following form:

$$\text{Im}\left[\frac{-1}{\varepsilon(W, q)}\right]_{\text{Ritchie}} = \sum_i A_i D_i(W, q; E_i, \gamma_i) \quad (6)$$

with A_i being (non-dispersive) weighting factors for each Drude peak. Connection to optical data is now made by the condition: $\text{Im}[-1/\varepsilon(W, q = 0)]_{\text{model}} \approx \text{Im}[-1/\varepsilon(W, q \approx 0)]_{\text{exp}}$. In both versions the fit to the optical data is made under the constraint of the f -sum rule (Smith 1985, Tanuma et al. 1993):

$$\int_0^\infty W \text{Im}[\varepsilon(W, q = 0)] dW = \int_0^\infty W \text{Im}\left[\frac{-1}{\varepsilon(W, q = 0)}\right] dW = \frac{\pi}{2} E_{pl}^2 \quad (7)$$

The extrapolation of the Drude coefficients $\{E_p, \gamma_i\}$ to $q \neq 0$ is made via dispersion relations commonly based on the random phase approximation (RPA) of the EG theory. To that end, an important property of the extended-Drude function Eq. (4) is that it fulfills the sum rule Eq. (7), *independent of the dispersion relations*, as long as it fulfills it at $q = 0$. Thus,

the form of the dispersion is to our disposal. According to the RPA, we can write:

$$E_i(q) = E_i + \alpha_{\text{RPA}} \frac{q^2}{2m_e} \approx E_i + \frac{q^2}{2m_e} \quad (8)$$

where m_e is the electron rest mass and α_{RPA} is the quadratic dispersion coefficient of the RPA. For liquid water $\alpha_{\text{RPA}} \approx 1$ to within a few percent (Emfietzoglou et al. 2009). The quadratic dispersion relation Eq. (8) approximates the dispersion of the EG at small- q while reproducing the Bethe ridge at high- q . In RPA plasmons are undamped at small- q . Therefore, it is commonly assumed that the damping constants do not disperse, i.e., $\gamma_i(q) = \gamma_i$.

Despite its simplicity, the application of Ritchie’s extended-Drude model can be laborious due to the large number of Drude functions often required to obtain a good fit of the optical data. The models of Penn (1987) and Ashley (1988) overcome the need for a parametric fit by replacing the summation over a finite number of extended-Drude functions (see Eq. 6) by an integration over a model ELF. Their origin can be traced to the EG statistical model of Tung et al. (1979). In the Penn model one writes:

$$\text{Im}\left[\frac{-1}{\varepsilon(W, q)}\right]_{\text{Penn}} = \int_0^\infty A(E_{pl}) \text{Im}\left[\frac{-1}{\varepsilon_L(W, q; E_{pl})}\right] dE_{pl} \quad (9)$$

where the weighting factors A_i of Eq. (6) have transformed to a spectrum density function $A(E_{pl})$ and the ELF of the Lindhard dielectric function $\varepsilon_L(W, q; E_{pl})$ replaces the Drude functions of Eq. (6). It is straightforward to show that connection with the optical data is made through:

$$A(W) = \frac{2}{\pi W} \text{Im}\left[\frac{-1}{\varepsilon(W, q \approx 0)}\right]_{\text{exp}} \quad (10)$$

The use of the *full* Lindhard dielectric function (Lindhard 1954) in the Penn model results in a substantial amount of numerical work. An important simplification is offered by the Ashley model which makes use of the one-mode approximation to the Lindhard-ELF leading to the strikingly simple expression:

$$\text{Im}\left[\frac{-1}{\varepsilon(W, q)}\right]_{\text{Ashley}} = \frac{W-Q}{W} \text{Im}\left[\frac{-1}{\varepsilon(W-Q, q \approx 0)}\right]_{\text{exp}} \Theta(W-Q) \quad (11)$$

with $Q = q^2/2m_e$. Historically, it appears that the first documentation of Ashley’s model (Ashley 1983) has preceded the publication of the Penn model (Penn 1987). Note that in both models, Eqs. (9) and (11), the f -sum rule is satisfied for all q as long as it is satisfied at $q = 0$. An approach that simplifies the numerical work of the Penn model while still reproducing the results of the Lindhard theory without resorting to Ashley’s one-mode approximation, is the two-mode model of Fernández-Varea et al. (1992, 1993). To the best of our knowledge, this model has not yet been applied to liquid water, perhaps owing to the extra effort required in optimizing some model parameters. As mentioned, all

EG-based extension models (discussed above) are not very accurate for inner-shell electrons which have binding energies often comparable to incident electron energies. For inner-shells the extension algorithm of Liljequist (1983, 1985) appears to be the most reliable.

New developments

Dingfelder et al. (1998) revisited the 1975 version of the Ritchie model and suggested a new parameterization scheme for representing the optical data (i.e., effective at $q = 0$) with improved properties near the ionization threshold. In particular, they introduced the ‘truncated’ Drude function for ionization collisions which reads:

$$D_i(W, q=0; E_i, \gamma_i) = \int_{E_i-\Delta_i}^{E_i+\Delta_i} \frac{W \gamma_i}{(\Omega^2 - W^2)^2 + (W \gamma_i)^2} \exp\left\{-\frac{(\Omega - E_i)^2}{2\Delta_i^2}\right\} \Theta(W - \Omega) d\Omega \quad (12)$$

where $\Theta()$ denotes the step function and Δ_i an empirically determined band width. To describe the excitations, those authors employed a sum of derivative Drude functions. Extension to $q \neq 0$ was still made by the replacement $E_i \rightarrow E_i(q)$ using Eq. (8) and the assumption of non-dispersive damping constants. This scheme was shown (Dingfelder and Inokuti 1999) to reproduce the global features of the experimental Bethe surface obtained via the IXS measurements. However, certain features remain beyond the capabilities of the model, most notably, its Bethe ridge has a width that is too small and a height that is too large. In an effort to improve this state of affairs, Emfietzoglou et al. (2005) parameterized the IXS data for the imaginary part of the dielectric function at $q = 0$ using a sum of normal and derivative Drude functions to represent the ionizations and excitations, respectively, and proposed new dispersion relations for $E_i(q)$ and $\gamma_i(q)$ to better comply with the experimental ELF at $q \neq 0$. The Emfietzoglou-Cucinotta-Nikjoo (ECN) empirical dispersion relations read:

$$E_i(q) = E_i + g(q) \frac{q^2}{2m_e} \quad (13)$$

where $g(q) = 1 - \exp(-cq^d)$ and

$$\gamma_i(q) = \gamma_i + aq + bq^2 \quad (14)$$

The values of the constants (a, b, c, d) depend little upon the parameterization of the optical data (Abril et al. 2010, Emfietzoglou et al. 2005). The effect of $g(q)$ is to reduce $E_i(q)$ at not too large q , thus, *shifting* the ELF to lower excitation energies while the q -dependent damping constant leads to the *broadening* of ELF. In the context of EG theory, this shifting and broadening of ELF is a direct outcome of (short-range) electron correlation and exchange effects (not considered within RPA) and theoretically predicted by the so-called many-body local field correction (LFC). To account for general momentum broadening effects in ELF Ritchie has suggested using the following simple dispersion relation for the damping constant (Dingfelder et al. 2008):

$$\gamma_i(q) = \gamma_i + \text{Ry}q \quad (15)$$

where $1 \text{ Ry} = 13.6 \text{ eV}$. Yet another approach has been presented by Garcia-Molina and co-workers (Emfietzoglou et al. 2008) who applied the MELF model (Abril et al. 1998) to liquid water. In the MELF model the extended-Drude functions in Eq. (6) are replaced by Mermin energy-loss functions (MELF):

$$\text{Im} \left[\frac{-1}{\epsilon(W, q)} \right]_{\text{MELF}} = \sum_i \frac{A_i}{E_i^2} \text{Im} \left[\frac{-1}{\epsilon_M(W, q; E_i, \gamma_i)} \right] \quad (16)$$

where $\epsilon_M(W, q; E_i, \gamma_i)$ denotes the Mermin dielectric function defined via an appropriate combination of terms that include $\epsilon_L(\tilde{W}, q; E_{pl})$ with $\tilde{W} = W + i\gamma$ (Mermin 1970). Thus, contrary to the Lindhard dielectric function $\epsilon_L(W, q; E_{pl})$ used in the Penn model which assumes an undamped plasmon at small q , damping is included into the Mermin dielectric function at all q .

Results

In Figure 1 we present the ELF of liquid water at $q = 0$ as obtained from the reflectance (REF) and IXS data. Also depicted are a parameterized Drude model (Emfietzoglou and Nikjoo 2005) and recent time-dependent density functional theory (TDDFT) calculations by Tavernelli (2006).

To investigate the influence of the two experimental optical data sets on the inelastic electron scattering cross section Λ , we have calculated from Eq. (1) whereby the ELF at $q = 0$ is determined by the two Drude model parameterizations depicted in Figure 1 representing the REF and IXS data, respectively. The extension of the ELF to $q \neq 0$ is done in the same way in both sets of calculations.

A comparison of the various methods discussed for extrapolating the optical data to $q \neq 0$ against the IXS data is presented in Figure 2 for two values of q . To investigate the effect on the inelastic electron scattering cross section of the different extension algorithms (or dispersion relations),

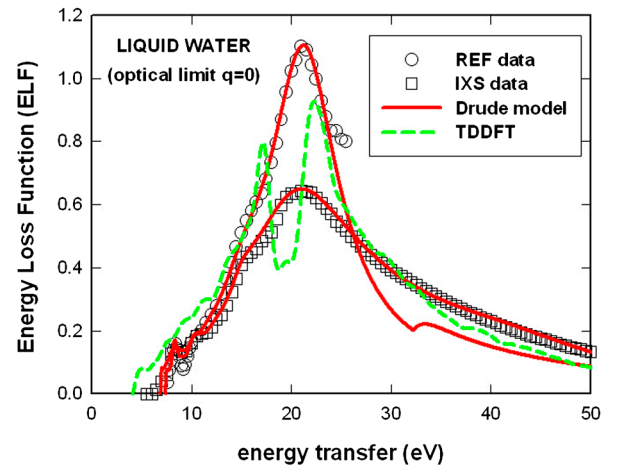


Figure 1. Experimental optical data obtained via reflectance (REF) measurements (Heller et al. 1974) and inelastic X-ray scattering (IXS) spectroscopy (Hayashi et al. 2000) are compared to *ab initio* time-dependent density functional theory (TDDFT) calculations (Tavernelli 2006) and a Drude model parameterization (Emfietzoglou and Nikjoo 2005).

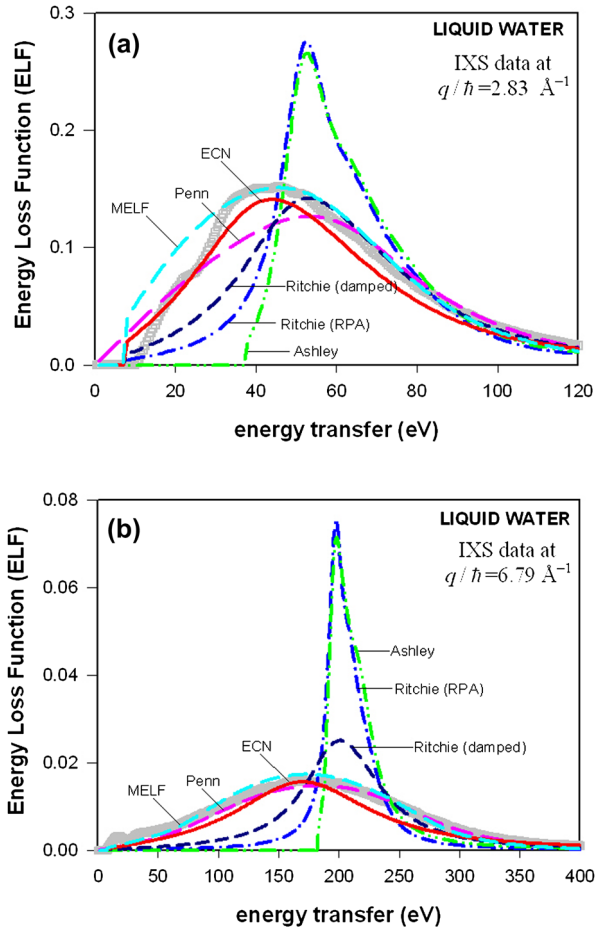


Figure 2. Experimental data (symbols) for the energy-loss function of liquid water obtained from IXS (Watanabe et al. 2000) at two different values of momentum transfer q are compared against different optical-data models which use the IXS optical data for $q = 0$ (Hayashi et al. 2000) but different extension algorithms to extrapolate them to $q \neq 0$ (for details on the models see the text). Panel (a) momentum transfer value $q/\hbar = 2.83 \text{ \AA}^{-1}$ or $q = 1.50 \text{ a.u.}$; panel (b) momentum transfer value $q/\hbar = 6.79 \text{ \AA}^{-1}$ or $q = 3.59 \text{ a.u.}$

we present in Figure 3 calculations of Λ via Eq. (1) using different representation of ELF at $q \neq 0$ but the same representation at $q = 0$. Specifically, the optical limit of ELF is based on the Drude model parameterization of the IXS data depicted in Figure 1 which satisfies the f -sum rule to within 1%.

Discussion

It is evident from Figure 1 that although the shape of the ELF predicted by both sets of data (REF, IXS) is similar, there is a sizeable disagreement with respect to the intensity of the main excitation peak at $\sim 21 \text{ eV}$. Specifically, in the IXS data the peak intensity is reduced by a factor of 1.5 compared to the REF data. A reduction of that magnitude has also been observed in the spectrum of water ice in both its hexagonal and amorphous form (Kobayashi 1983). This has often been used as an argument in favour of the IXS data, especially, in view of the fact that amorphous ice has a similar molecular layout to liquid water.

With respect to the influence of the two optical data sets on the inelastic electron scattering cross section, Λ , it was found that the IXS data lead to smaller Λ values by 5–10% in

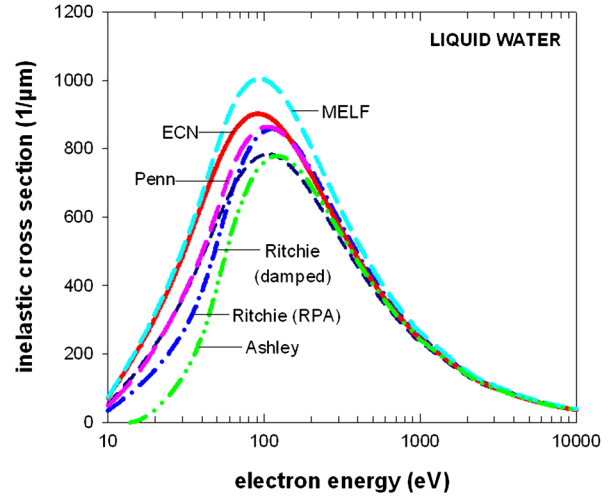


Figure 3. The total inelastic scattering cross section as a function of electron energy calculated by different optical-data models which use the IXS optical data for $q = 0$ (Hayashi et al. 2000) but different extension algorithms to extrapolate them to $q \neq 0$: Ritchie (RPA) model (Ritchie and Howie 1977), Penn model (Penn 1987), Ashley model (Ashley 1988), MELF model (Abril et al. 1998), ECN model (Emfietzoglou et al. 2005), and the Ritchie damped model (Dingfelder et al. 2008) (for details on the models see the text).

the electron energy range 200–10,000 eV and up to 25% in the range 50–200 eV. The difference increases further at very low energies, reaching 40% at 10 eV but, as already mentioned, optical-data model calculations below 50 eV may be only qualitative.

From the comparison presented in Figure 2 between the various extension algorithms and the IXS data follow several observations. First, it is evident that the use of the RPA dispersion in the Ritchie model results in a sharply-peaked ELF, a problem also shared by the Ashley model. The latter has the additional problem of a pseudo threshold at an energy transfer just below the plasmon energy. The sharp peak in both models is essentially due to the use of a non-dispersive damping constant. The Penn model, on the other hand, seems to predict well the observed broadening of the ELF. This might be surprising given that the Penn model uses the Lindhard dielectric function which assumes an infinite plasmon lifetime (i.e., neglects damping). However, even within RPA a strong momentum broadening effect is predicted for q above the Fermi value q_F ($q_F/\hbar \approx 2.27 \text{ \AA}^{-1}$ for liquid water) where plasmons can decay via individual single-particle excitations (Landau damping).

Concerning the new developments it is clear that although the ‘damped’ Ritchie model improves its RPA version, the overall agreement with the IXS data is still rather unsatisfactory. As a matter of fact, in the Ritchie and Ashley models at all q as well as in the Penn model at small q , the Bethe ridge appears somewhat displaced towards higher energy transfer. This is a fundamental problem with the RPA due to the neglect of (short-range) electron exchange and correlation effects which, in the context of EG theory, can be accounted for via the action of the many-body local field correction (LFC). This is a complex-valued function of energy- and momentum-transfer with its real part reducing

the plasmon energy from its RPA value (i.e., causing the Bethe ridge to move towards smaller energy transfer) and its imaginary part introducing plasmon damping (due to electron-electron collision effects in the electron gas). The ECN dispersion relations appear to improve considerably the agreement of the Ritchie models with the IXS data by accounting in an empirical manner for the shifting and broadening of the ELF. Likewise, the MELF model which also for accounts in a phenomenological, yet consistent manner, (short-range) electron exchange and correlation effects in screening (at all q) via the Mermin dielectric function, provides a fairly good representation of the IXS data.

With respect to the effect of the extension algorithm upon the inelastic electron scattering cross section, Λ , it can be seen from Figure 3 that the use of different extension algorithms becomes more and more important with decreasing electron energy. Differences among the models is only $\sim 5\%$ in the energy range 200–10,000 eV but it increases rapidly at lower electron energies reaching a factor of 2 in the range 50–200 eV (and even further at still lower energies). It is noteworthy that extension algorithms that do not account for the momentum broadening of ELF, such as the early Ritchie model(s) and the Ashley model, exhibit a much steeper fall below the maximum. Interestingly, the simple damped Ritchie model reproduces well (to within $\pm 10\%$) the more involved Penn model down to 10 eV. The ECN and MELF models result in the largest values, especially in the region of the maximum. The difference between the ECN and MELF calculations are less than $\sim 10\%$.

Conclusions

A short overview has been presented on the use of optical-data models for computing the inelastic scattering of low-energy electrons in liquid water. The inelastic scattering cross section was found to be rather insensitive (to within 10%) to the optical data and/or the model used to extend them to $q \neq 0$ for energies above 200 eV. Differences between models increase rapidly though below 200 eV where the calculations were found to depend more sensitively upon the extension algorithm than on the optical data used. The ECN and MELF models which account for effects beyond RPA, offer the best overall agreement with the IXS data at $q \neq 0$, thus, they presently seem to offer the most trustworthy approach below 200 eV. In that respect, it would be highly desirable to have a new set of measurements beyond the optical limit to confirm the IXS data which currently represent the only source of information. Similarly, efforts should be invested to the development of extension algorithms that will go beyond the RPA by considering the effect of (short range) electron exchange and correlation. Finally, we should highlight that the reliability of calculations below 200 eV may also depend upon effects not considered in the PWBA such as exchange and low-energy Coulomb corrections which have been discussed elsewhere (Dingfelder et al. 1998, Emfietzoglou and Nikjoo 2007, Fernández-Varea et al. 1993).

Acknowledgments

We thank I. Tavernelli for kindly allowing us to use the *ab initio* data depicted in Figure 1. Financial support for D.E. and I.K. by the European Union FP7 ANTICARB (HEALTH-F2-2008-201587) is acknowledged. I.A. and R.G.M. acknowledge financial support from the Spanish Ministerio de Ciencia e Innovación (Project FIS2010-17225). Work in HN group is supported by SSM (Swedish Radiation Safety Authority).

Declaration of interest

The authors report no conflicts of interest. The authors alone are responsible for the content and writing of the paper.

References

- Abril I, Garcia-Molina R, Denton CD, Pérez-Pérez JF, Arista NR, 1998. Dielectric description of wakes and stopping powers in solids. *Physical Review A* 58:357–366.
- Abril I, Denton CD, de Vera P, Kyriakou I, Emfietzoglou D, Garcia-Molina R. 2010. Effect of the Bethe surface description on the electronic excitations induced by energetic proton beams in liquid water and DNA. *Nuclear Instruments and Methods in Physics Research B: Beam Interactions with Materials & Atoms* 268: 1763–1767.
- Ashley JC. 1983. Simple model for calculating stopping powers of condensed organic materials for low-energy electrons. 7th International Congress on Radiation Research. Amsterdam, The Netherlands: Martinus Nijhoff Publishers. p. A1–O3.
- Ashley JC. 1988. Interaction of low-energy electrons with condensed matter: stopping powers and inelastic mean free paths from optical data. *Journal of Electron Spectroscopy and Related Phenomena* 46:199–214.
- Dingfelder M. 2006. Track structure: Time evolution from physics to chemistry. *Radiation Protection Dosimetry* 122:16–21.
- Dingfelder M, Hantke D, Inokuti M, Paretzke HG. 1998. Electron inelastic-scattering cross sections in liquid water. *Radiation Physics and Chemistry* 53:1–18.
- Dingfelder M, Inokuti M. 1999. The Bethe surface of liquid water. *Radiation and Environmental Biophysics* 38:93–96.
- Dingfelder M, Ritchie RH, Turner JE, Friedland W, Paretzke HG, Hamm RN. 2008. Comparisons of calculations with PARTRAC and NOREC: transport of electrons in liquid water. *Radiation Research* 169:584–594.
- Emfietzoglou D., Nikjoo H. 2005. The effect of model approximations on single-collision distributions of low-energy electrons in liquid water. *Radiation Research* 163:98–111.
- Emfietzoglou D, Cucinotta F, Nikjoo H. 2005. A complete dielectric response model for liquid water: a solution of the Bethe ridge problem. *Radiation Research* 164:202–211.
- Emfietzoglou D, Nikjoo H. 2007. Accurate electron inelastic cross sections and stopping powers for liquid water over the 0.1–10 keV range based on an improved dielectric description of the Bethe surface. *Radiation Research* 167:110–120.
- Emfietzoglou D, Abril I, Garcia-Molina R, Petsalakis ID, Nikjoo H, Kyriakou I, Pathak A. 2008. Semi-empirical dielectric descriptions of the Bethe surface of the valence bands of condensed water. *Nuclear Instruments and Methods in Physics Research B: Beam Interactions with Materials & Atoms* 266:1154–1161.
- Emfietzoglou D, Garcia-Molina R, Kyriakou I, Abril I, Nikjoo H. 2009. A dielectric response study of the electronic stopping power of liquid water for energetic protons and a new I -value for water. *Physics in Medicine and Biology* 54:3451–3472.
- Fermi E. 1940. The ionization loss of energy in gases and in condensed materials. *Physical Review* 57:485–493.
- Fernández-Varea JM, Mayol R, Salvat F, Liljequist D. 1992. A comparison of inelastic scattering models based on a δ -function representation of the Bethe surface. *Journal of Physics: Condensed Matter* 4: 2879–2890.
- Fernández-Varea JM, Mayol R, Liljequist D, Salvat F. 1993. Inelastic scattering of electrons in solids from a generalized oscillator strength

- model using optical and photoelectric data. *Journal of Physics: Condensed Matter* 5:3593–3610.
- Fernández-Varea JM, Llovet X, Salvat F. 2005a. Cross sections for electron interactions in condensed matter. *Surface and Interface Analysis* 37:824–832.
- Fernández-Varea JM, Salvat F, Dingfelder M, Liljequist D. 2005b. A relativistic optical-data model for inelastic scattering of electrons and positrons in condensed matter. *Nuclear Instruments and Methods in Physics Research B: Beam Interactions with Materials & Atoms* 229:187–218.
- Hamm RN, Wright HA, Ritchie RH, Turner JE, Turner TP. 1975. Monte Carlo transport of electrons through liquid water. 5th Symposium on Microdosimetry. Brussels: EUR-5452 EC. pp. 1037–1050.
- Hayashi H, Watanabe N, Udagawa Y, Kao CC. 2000. The complete optical spectrum of liquid water measured by inelastic x-ray scattering. *Proceedings of the National Academy of Science of USA* 97:6264–6266.
- Heller JM, Hamm RN, Birkhoff RD, Painter LR. 1974. Collective oscillation in liquid water. *Journal of Chemical Physics* 60:3483–3486.
- Inokuti M. 1971. Inelastic collisions of fast charged particles with atoms and molecules – The Bethe theory revisited. *Reviews of Modern Physics* 43:297–347.
- Kobayashi K. 1983. Optical spectra and electronic structure of ice. *Journal of Physical Chemistry* 87:4317–4321.
- Liljequist D. 1983. A simple calculation of inelastic mean free path and stopping power for 50 eV–50 keV electrons in solids. *Journal of Physics D: Applied Physics* 16:1567–1582.
- Liljequist D. 1985. Simple generalized oscillator strength density model applied to the simulation of keV electron-energy-loss distributions. *Journal of Applied Physics* 57:657–665.
- Lindhard J. 1954. On the properties of a gas of charged particles. *Det Kongelige Danske Videnskabernes Selskab Matematisk-fysiske Meddelelser* 28:1–57.
- Mermin ND. 1970. Lindhard dielectric function in the relaxation-time approximation. *Physical Review B* 1:2362–2363.
- Penn DR. 1987. Electron mean-free-path calculations using a model dielectric function. *Physical Review B* 35:482–486.
- Powell CJ. 1967. Inelastic scattering of kilovolt electrons by solids and liquids: determination of energy losses, cross sections, and correlations with optical data. *Health Physics* 13:1265–1275.
- Powell CJ. 1974. Attenuation lengths of low-energy electrons in solids. *Surface Science* 44:29–46.
- Ritchie RH. 1959. Interaction of charged particles with a degenerate Fermi-Dirac electron gas. *Physical Review* 114:644–654.
- Ritchie RH, Howie A. 1977. Electron excitation and the optical potential in electron microscopy. *Philosophical Magazine* 36:463–481.
- Ritchie RH, Hamm RN, Turner JE, Wright HA. 1978. The interaction of swift electrons with liquid water. 6th Symposium on Microdosimetry. Brussels, Belgium: EUR-6064 EC. pp. 345–354.
- Ritchie RH, Hamm RN, Turner JE, Wright HA, Bloch WE. 1991. Radiation interactions and energy transport in the condensed phase. In: *Physical and Chemical Mechanisms in Molecular Radiation Biology*. New York: Plenum Press. pp. 99–133.
- Salvat F, Fernández-Varea JM. 2009. Overview of physical interaction models for photon and electron transport used in Monte Carlo codes. *Metrologia* 46:S112–S138.
- Smith DY. 1985. Dispersion theory, sum rules, and their application to the analysis of optical data. In E.D. Palik (ed.) *Handbook of optical constants of solids*. New York: Academic Press. pp. 35–68.
- Tanuma S, Powell CJ, Penn DR. 1993. Use of sum rules on the energy-loss function for the evaluation of experimental optical data. *Journal of Electron Spectroscopy and Related Phenomena* 62:95–109.
- Tanuma S, Powell CJ, Penn DR. 2011. Calculations of electron inelastic mean free paths IX. Data for 41 elemental solids over the 50 eV to 30 keV range. *Surface and Interface Analysis* 43:689–713.
- Tavernelli I. 2006. Electronic density response of liquid water using time-dependent density functional theory. *Physical Review B* 73:094204.
- Tung CJ, Ashley JC, Ritchie RH. 1979. Electron inelastic mean free paths and energy losses in solids II. Electron gas statistical model. *Surface Science* 81:427–439.
- Watanabe N, Hayashi H, Udagawa Y. 2000. Inelastic X-ray scattering study on molecular liquids. *Journal of Physics and Chemistry of Solids*. 61:407–409.